Plasmonically enhanced Faraday effect in metal and ferrite nanoparticles composite precipitated inside glass

Seisuke Nakashima,[1, 2, *] Koji Sugioka,[2] Katsuhisa Tanaka,[3] Masahiro Shimizu,[3] Yasuhiko Shimotsuma,[3] Kiyotaka Miura,[3] Katsumi Midorikawa,[2] and Kohki Mukai[1]

[1] *Department of Solid State Materials and Engineering, Graduate School of Engineering, Yokohama National University, 79-5 Tokiwadai, Hodogaya-ku, Yokohama, Kanagawa 240-8501, Japan*
[2] *RIKEN – Advanced Research Institute, 2-1 Hirosawa, Wako, Saitama 351-0198, Japan*
[3] *Department of Material Chemistry, Graduate School of Engineering, Kyoto University, Kyotodaigakukatsura, Nishikyo-ku, Kyoto, Kyoto 615-8510, Japan*
nakashima@ynu.ac.jp

Abstract: Using femtosecond laser irradiation and subsequent annealing, nanocomposite structures composed of spinel-type ferrimagnetic nanoparticles (NPs) and plasmonic metallic NPs have been formed space-selectively within glass doped with both α-Fe_2O_3 and Al. The Faraday rotation spectra exhibit a distinct negative peak at around 400 nm, suggesting that the ferrimagnetic Faraday response is enhanced by the localized surface plasmon resonance (LSPR) due to metallic Al NPs. At the interfaces in the nanocomposites, the ferrimagnetism of magnetite NPs is directly coupled with the plasmon in the Al NPs. The control of the resonance wavelength of the magneto-optical peaks, namely, the size of plasmonic NPs has been demonstrated by changing the irradiation or annealing conditions.

OCIS codes: (160.3820) Magneto-optical materials; (320.7090) Ultrafast lasers; (250.5403) Plasmonics; (350.3390) Laser materials processing.

References and links

1. G. B. Scott, D. E. Lacklison, H. I. Ralph, and J. L. Page, "Magnetic circular dichroism and Faraday rotation spectra of $Y_3Fe_5O_{12}$," Phys. Rev. B **12**(7), 2562–2571 (1975).
2. P. K. Jain, Y. H. Xiao, R. Walsworth, and A. E. Cohen, "Surface plasmon resonance enhanced magneto-optics (SuPREMO): Faraday rotation enhancement in gold-coated iron oxide nanocrystals," Nano Lett. **9**(4), 1644–1650 (2009).
3. L. Wang, C. Clavero, Z. Huba, K. J. Carroll, E. E. Carpenter, D. F. Gu, and R. A. Lukaszew, "Plasmonics and enhanced magneto-optics in core-shell Co-Ag nanoparticles," Nano Lett. **11**(3), 1237–1240 (2011).
4. C. S. Levin, C. Hofmann, T. A. Ali, A. T. Kelly, E. Morosan, P. Nordlander, K. H. Whitmire, and N. J. Halas, "Magnetic-plasmonic core-shell nanoparticles," ACS Nano **3**(6), 1379–1388 (2009).
5. Y. Q. Li, Q. Zhang, A. V. Nurmikko, and S. H. Sun, "Enhanced magnetooptical response in dumbbell-like Ag-CoFe2O4 nanoparticle pairs," Nano Lett. **5**(9), 1689–1692 (2005).
6. C. Wang, C. J. Xu, H. Zeng, and S. H. Sun, "Recent progress in syntheses and applications of dumbbell-like nanoparticles," Adv. Mater. (Deerfield Beach Fla.) **21**(30), 3045–3052 (2009).
7. R. Fujikawa, A. V. Baryshev, J. Kim, H. Uchida, and M. Inoue, "Contribution of the surface plasmon resonance to optical and magneto-optical properties of a Bi: YIG-Au nanostructure," J. Appl. Phys. **103**(7), 07D301-303 (2008).
8. S. Ozaki, H. Kura, H. Maki, and T. Sato, "Manipulation of Faraday rotation in Bi-substituted yttrium-iron garnet film using electromagnetic interaction between Au nanoparticles in two-dimensional array," J. Appl. Phys. **106**(12), 123530 (2009).
9. Y. P. Lee, Y. V. Kudryavtsev, V. V. Nemoshkalenko, R. Gontarz, and J. Y. Rhee, "Magneto-optical and optical properties of Fe-rich Au-Fe alloy films near the fcc-bcc structural transformation region," Phys. Rev. B **67**(10), 104424 (2003).
10. K. M. Davis, K. Miura, N. Sugimoto, and K. Hirao, "Writing waveguides in glass with a femtosecond laser," Opt. Lett. **21**(21), 1729–1731 (1996).
11. J. Lehmann, M. Merschdorf, W. Pfeiffer, A. Thon, S. Voll, and G. Gerber, "Surface plasmon dynamics in silver nanoparticles studied by femtosecond time-resolved photoemission," Phys. Rev. Lett. **85**(14), 2921–2924 (2000).

#173803 - $15.00 USD Received 3 Aug 2012; revised 9 Oct 2012; accepted 12 Oct 2012; published 5 Dec 2012

12. T. Tamaki, W. Watanabe, H. Nagai, M. Yoshida, J. Nishii, and K. Itoh, "Structural modification in fused silica by a femtosecond fiber laser at 1558 nm," Opt. Express **14**(15), 6971–6980 (2006).
13. Y. Shimotsuma, P. G. Kazansky, J. R. Qiu, and K. Hirao, "Self-organized nanogratings in glass irradiated by ultrashort light pulses," Phys. Rev. Lett. **91**(24), 247405 (2003).
14. S. Nakashima, K. Fujita, A. Nakao, K. Tanaka, Y. Shimotsuma, K. Miura, and K. Hirao, "Enhanced magnetization and ferrimagnetic behavior of normal spinel ZnFe(2)O(4) thin film irradiated with femtosecond laser," Appl. Phys., A Mater. Sci. Process. **94**(1), 83–88 (2009).
15. K. Miura, J. R. Qiu, H. Inouye, T. Mitsuyu, and K. Hirao, "Photowritten optical waveguides in various glasses with ultrashort pulse laser," Appl. Phys. Lett. **71**(23), 3329–3331 (1997).
16. K. Sugioka, Y. Cheng, and K. Midorikawa, "Three-dimensional micromachining of glass using femtosecond laser for lab-on-a-chip device manufacture," Appl. Phys., A Mater. Sci. Process. **81**(1), 1–10 (2005).
17. K. Sugioka, Y. Hanada, and K. Midorikawa, "Three-dimensional femtosecond laser micromachining of photosensitive glass for biomicrochips," Laser Photon. Rev. **4**(3), 386–400 (2010).
18. J. R. Qiu, M. Shirai, T. Nakaya, J. H. Si, X. W. Jiang, C. S. Zhu, and K. Hirao, "Space-selective precipitation of metal nanoparticles inside glasses," Appl. Phys. Lett. **81**(16), 3040–3042 (2002).
19. J. R. Qiu, X. W. Jiang, C. S. Zhu, H. Inouye, J. H. Si, and K. Hirao, "Optical properties of structurally modified glasses doped with gold ions," Opt. Lett. **29**(4), 370–372 (2004).
20. K. Miura, K. Hirao, Y. Shimotsuma, M. Sakakura, and S. Kanehira, "Formation of Si structure in glass with a femtosecond laser," Appl. Phys., A Mater. Sci. Process. **93**(1), 183–188 (2008).
21. S. Nakashima, K. Sugioka, and K. Midorikawa, "Space-selective modification of the magnetic properties of transparent Fe3+-doped glass by femtosecond-laser irradiation," Appl. Phys., A Mater. Sci. Process. **104**(3), 993–996 (2011).
22. A. Bishay, "Radiation induced color centers in multicomponent glasses," J. Non-Cryst. Solids **3**(1), 54–114 (1970).
23. G. H. Chan, J. Zhao, G. C. Schatz, and R. P. V. Duyne, "Localized surface plasmon resonance spectroscopy of triangular aluminum nanoparticles," J. Phys. Chem. C **112**(36), 13958–13963 (2008).

1. Introduction

Nanocomposites or nanostructures that combine plasmonic metal nanoparticles (NPs) and ferromagnetic NPs are promising material systems from both practical and fundamental viewpoints due to the localized surface plasmon enhancement of magneto-optical responses, such as Faraday and Kerr rotations. Magneto-optical responses, which provide detailed physical information on the electronic and spin structure of materials [1], are enhanced by the plasmonically excited electric field that arises in the interfacial region between the metallic and magnetic NPs. Recent advances include the discovery of such enhancement phenomena in core-shell nanocrystals [2–4], dumbbell-like nanoparticle pairs [5, 6], plasmonic NPs deposited on ferrimagnetic thin films [7], and ferromagnetic/plasmonic multilayer structures [8]. The advantage of nanocomposite materials lies not only in their much higher efficiency compared to ferromagnetic metal alloys [9] but also the high flexibility and controllability of their composition, which make it possible to optimize their magnetism and the plasmonic properties, respectively.

In general, chemical synthesis or vapor deposition is the most popular method for preparing nanocomposite materials. However, synthesized colloidal NPs are stable only in the presence of synthetic solvents. Therefore, it is difficult to fabricate complicated three-dimensional structures or superlattices for application to nanosized magneto-optical devices by stacking the dried NPs. In this paper, a novel method is proposed for preparing plasmonic and magneto-optical nanoparticle composites and for 3-dimensional structuring, based on space-selective precipitation inside transparent glass using high-intensity ultrashort laser pulses, such as those produced by a femtosecond- (fs-) laser. Femtosecond-lasers are widely recognized as powerful tools for sensing the optical properties of materials, or space-selectively modifying their optical, electrical, mechanical, or magnetic properties [10–17]. Focusing an fs-laser inside a transparent glass locally induces a variety of interactions with atoms, such as photoreduction, photoexcitation, heat accumulation, and atomic diffusion based on nonlinear multiphoton absorption. In addition, there have been many reports of post-annealing processes following irradiation giving rise to the space-selective precipitation of metallic or oxide NPs [18–20]. Recently, we have also succeeded in modifying the local magnetism in a Fe-oxide-doped glass using an fs-laser process [21]. The ferrimagnetic spinel-type crystalline phase, magnetite, was successfully produced by irradiation with an fs-laser and subsequent annealing. The room-temperature magnetization was manifestly enhanced

#173803 - $15.00 USD Received 3 Aug 2012; revised 9 Oct 2012; accepted 12 Oct 2012; published 5 Dec 2012

compared with that of the non-irradiated glass. These experiments represent the first direct observation of space-selective laser-induced precipitation of the ferrimagnetic phase. A further challenge would be the ability to cause simultaneous precipitation of magnetic and plasmonic metal NPs. Since the modified region is spatially confined to an area corresponding to the spot size of the focused laser pulse, it might be expected that nanoparticle pairs with magnetic and plasmonic crystalline phases would precipitate. In the present study, the effect of fs-laser irradiation on the optical, magnetic, and magneto-optical properties of soda lime silicate glass doped with both Fe oxide (hematite; α-Fe_2O_3) and Al was investigated.

2. Experimental

Soda lime silicate glass doped with α-Fe_2O_3 and Al was prepared by melt-quenching. The glass composition was $0.05Fe_2O_3 \cdot 0.1Al \cdot 70SiO_2 \cdot 20Na_2O \cdot 10CaO$ (mol/%). Reagent-grade SiO_2, Na_2CO_3, $CaCO_3$, Fe_2O_3, and Al were used as starting materials. A mixture of these powders was melted in a platinum crucible at 1550 °C for 1 h in air. The melt was then quenched into a transparent glass by casting it onto a stainless-steel plate at room temperature. The glass was cut and both sides were polished to obtain 3-mm-thick samples.

To irradiate the samples, a near-infrared fs-laser (Clark-MXR, CPA-2001) with a center wavelength of 775 nm, a pulse width of 150 fs (full width at half maximum), and a repetition rate of 1 kHz was used. The laser beam passing through a 3-mm-diameter aperture was focused 1 mm below the glass surface using a × 20 microscope objective with a numerical aperture of 0.46 to produce a 2.68-μm-diameter spot. The pulse energy was set at 20 μJ/pulse and was focused. The glass samples were placed horizontally on a PC-controlled *XY* stage and translated in the *X* direction at a speed of 1000 μm/s. The laser beam was alternately scanned back and forward with a pitch of 5 μm in the *Y* direction, producing a square irradiated area with 4-mm-long sides. After laser irradiation, the glass samples were annealed in air under various temperature and duration time. The annealing was started by introducing the samples into the furnace maintained at the annealing temperature. Then, their absorption spectra were measured using a spectrophotometer (JASCO V-570) in the wavelength range from 200 to 1000 nm.

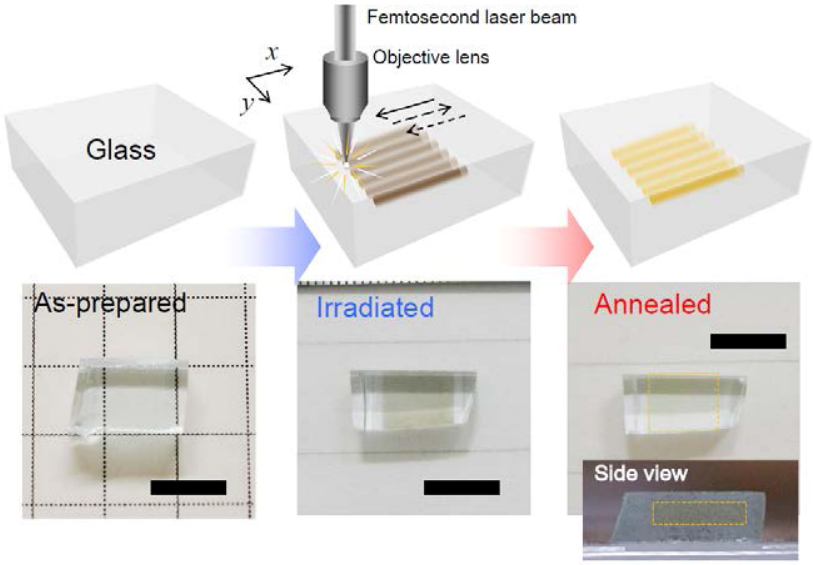

Fig. 1. Schematic procedure for laser-irradiation processes and optical micrograph images for each step. The scale bars represent 5 mm.

#173803 - $15.00 USD Received 3 Aug 2012; revised 9 Oct 2012; accepted 12 Oct 2012; published 5 Dec 2012

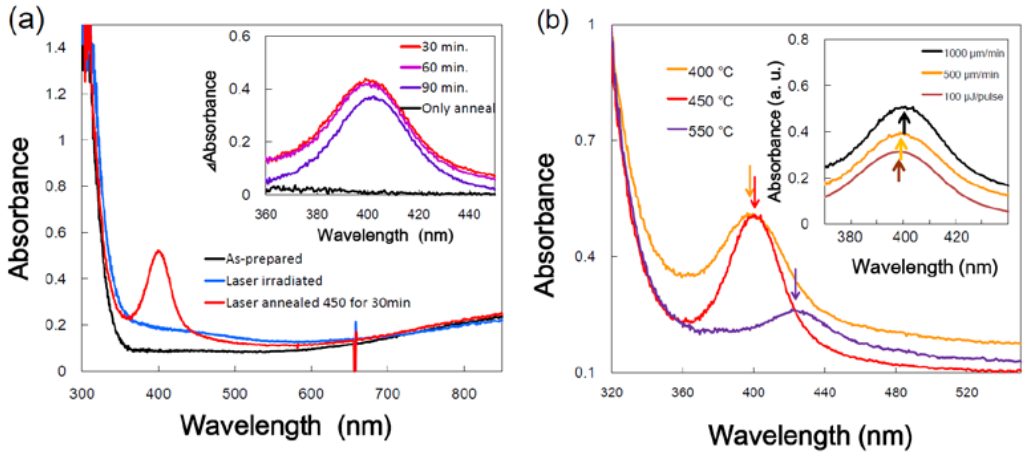

Fig. 2. (a) Optical absorption spectra of the as-prepared (black curve), irradiated (blue curve), and annealed (red curve) glass samples. The inset shows spectra of the samples annealed at 450 °C for 30, 60, and 90 min. (b) Absorption spectra of the glass samples irradiated and annealed at 400, 450, and 550 °C. The inset shows spectra of the samples irradiated at the scanning speed of 1000 and 500 μm/min and the glass irradiated at the pulse energy of 100 μJ/pulse.

3. Results and discussion

The as-prepared glass doped with α-Fe_2O_3 and Al was highly transparent, as shown in the left-side photograph in Fig. 1. Figure 2(a) shows the absorption spectra of the as-prepared (black curve), irradiated (blue curve), and annealed (red curve) glass samples. The as-prepared glass was highly transparent at visible wavelengths (i.e., longer than 340 nm). This is ascribable to the small absorption cross section of trivalent Fe ions, since all *d-d* transitions are spin forbidden in the high-spin configuration. We also found a relatively high absorption in the near-infrared region longer than 800 nm compared with glass doped only with α-Fe_2O_3, as was reported in a previous paper [21]. It is speculated that this absorption stems from a small amount of reduction of Fe ions due to the presence of Al.

The color of the fs-laser irradiated region in the glass changed to dark brown, as shown in the central photograph in Fig. 1. This corresponds to broad absorption peaks at around 430 and 620 nm (Fig. 2(a)), which can be attributed to hole-trap centers (e.g., HC_1 and HC_2) at nonbridging oxygens. HC_1 and HC_2 represent holes trapped in SiO_4 polyhedra with two and three nonbridging oxygens, respectively [10, 19, 22]. In the present case, free electrons are driven from the 2*p* orbital of the nonbridging oxygen due to multiphoton absorption of the incident photons. Neighboring Fe^{3+} ions are then partially reduced to Fe^{2+} ions by trapping the free electrons [19]. This is quite similar to the situation for glass doped only with α-Fe_2O_3.

In the subsequent annealling process at 450 °C, however, the irradiated brown region became faint yellow, as shown in the right-side photograph in Fig. 1. In the absorption spectrum, a distinct peak emerges at about 400 nm, and is assumed to correspond to localized surface plasmon resonance (LSPR) absorption due to metal NPs. The inset in Fig. 2(a) shows the change in the appearance of this peak as the annealing time increases from 30 to 90 min. It can be seen that with increasing annealing time, the absorption peak exhibits a small red shift from 399.15 to 401.91 nm. A red shift was also observed as the annealing temperature was increased, as shown in Fig. 2(b) for an annealing time of 30 min. Thus, it is clear that increasing either the duration or temperature of the anneal promotes the growth of crystalline NPs. On the other hand, when the laser beam was scanned more slowly, so that the irradiation dose was higher, the absorption peak shifted to shorter wavelength, as shown in the inset of Fig. 2(b). At a higher irradiation dose, the number of metal NP nucleation events would increase, leading to a lower growth rate of NPs in the annealing process, and thus smaller

#173803 - $15.00 USD Received 3 Aug 2012; revised 9 Oct 2012; accepted 12 Oct 2012; published 5 Dec 2012

particles sizes. In the case of higher pulse energy (100 μJ/pulse), the LSPR absorption peak revealed a blue shift due to the similar situation. The observed spectral features can therefore be well explained in terms of LSPR absorption due to metal NPs.

Meanwhile, the possibility of Fe NPs can be excluded because the plasma resonant frequency for Fe is in the infrared region. It is therefore proposed that the origin of the plasmon resonance is Al nanoparticles. Miura and his associates have reported that fs-laser irradiation can induce atomic diffusion of Al atoms inside glass materials [20]. In the region surrounding the focal point, a high concentration of Al can accumulate, and it is expected that additional annealing following irradiation would cause precipitation of Al nanocrystals. Meanwhile, Chan has reported that Al nanostructures with sizes of about 50 nm grown on glass substrates exhibit LSPR absorption at a wavelength of 390 nm, which is shorter than that for NPs made from noble metal, such as Au or Ag [23] and almost equivalent to the absorption observed in this study.

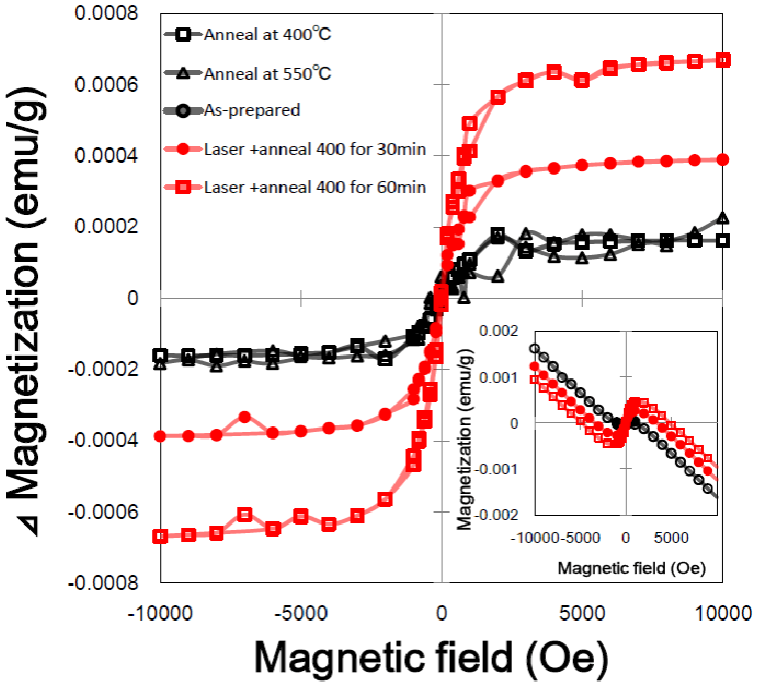

Fig. 3. Inset shows external magnetic field dependences of magnetization at room temperature for as-prepared (black open circles), irradiated and annealed at 400 °C for 30 min (red closed circles), and for 60 min (red open squares). Differences in magnetization between as-prepared and irradiated samples were compared with the samples singly annealed at 400 (black open squares) and 550 °C (black open triangle).

The room-temperature magnetization as a function of external magnetic field was next evaluated for each sample using a superconducting quantum interference device magnetometer (Quantum Design, MPMS-XL). The inset in Fig. 3 shows raw magnetization data for the as-prepared samples (black open circles), samples irradiated and annealed at 450 °C for 30 min (red closed circles), and irradiated and annealed at 450 °C for 60 min (red open squares) samples. Amorphous oxide glasses homogeneously doped with Fe are basically paramagnetic at room temperature because of the weak magnetic interactions. However, the as-prepared sample had a very low saturation magnetization, M_s. This contribution is negligible, and is probably attributable to local magnetic interactions among slightly aggregated trivalent Fe ions. Meanwhile, the irradiated and annealed samples show M_s values significantly larger than the as-prepared sample due to ferromagnetic contributions. Based on the assumption that these contributions are entirely saturated at high magnetic fields, the

#173803 - $15.00 USD Received 3 Aug 2012; revised 9 Oct 2012; accepted 12 Oct 2012; published 5 Dec 2012

linear diamagnetic components with negative gradients due to the non-magnetic glass matrix were subtracted as the background. The curves shown in the main plot in Fig. 3 represent the difference in magnetization between the as-prepared and the irradiated samples following background subtraction. The curves for unirradiated samples annealed at 450 °C (black open squares) and 550 °C (black open triangles) for 30 min were also shown. The increase in M_s for the irradiated and annealed samples is much larger than that for the annealed-only samples, implying that fs-laser irradiation plays an important role in the enhancement of the magnetization. As discussed in our previous paper, the estimated M_s values are not accurate, because the contributions of unirradiated areas are also included in this estimation [21]. Assuming that the change in the magnetization is restricted to the vicinity of the focal region (colored region), the enhancement factor is calculated to be at least nine times. This is almost equivalent to that for glass materials doped with only α-Fe_2O_3. Therefore, the magnetization enhancement effect is predominantly related to the presence of Fe ions. In other words, it is independent of the presence of Al. The coercive field is estimated to be 33 Oe, suggesting superparamagnetic behavior due to the presence of ferrimagnetic nanocrystals distantly dispersed in the diamagnetic glass matrix. Taking into account the results of our previous study, it is considered that ferrimagnetic magnetite NPs with a spinel structure. When the sample was irradiated with a fs-laser beam, free electrons were generated and holes were trapped on the nonbridging oxygens. At the same time, atomic diffusion of Fe ions occurs due to the heat gradient generated near the focal point [18], producing local regions with high Fe concentrations. In these regions, crystalline phase would be easily formed by external thermal stimulation, such as annealing. Then, the free electrons can reduce trivalent Fe ions to divalent ions. Due to the coexistence of Fe^{3+} and Fe^{2+}, ferrimagnetic magnetite NPs were precipitated as the most stable crystalline phase. That is why the glass sample shows an enhanced magnetization and superparamagnetic behaviors [21].

Nanostructures at the irradiated area in the glass were directly imaged by transmission electron microscopy (TEM) using a JEOL JEM2100F at 200 kV. As shown in the bright-field TEM images of the glass irradiated and then annealed at 550 °C for 30 min (Fig. 4(a)), nanocomposite structures consisting of two different NPs can be observed. It is speculated that the smaller ones with dark contrast (2-4 nm) correspond to the metallic Al phase which exhibit LSPR absorption at around 400 nm. The lighter contrast regions, which exhibit clear lattice fringes, represent larger particles of ferrimagnetic magnetite with diameters of about 5-7 nm. The nucleation and the following growth of each crystalline NPs are simultaneously induced by the irradiation and the subsequent annealing. As shown in Fig. 4(b), the plasmonic and magnetic NPs were adjacently precipitated in a spatially confined area due to the focused laser pulses, leading to creation of composite nanostructures of Al and magnetite NPs.

The obtained nanocomposites can be expected to exhibit a direct coupling between the magneto-optical response and plasmonic resonance at the grain boundaries [5–8]. The variations in the Faraday rotation angle as a function of wavelength were measured under the external magnetic field of 15 kOe using a commercially available measurement system for Faraday and Kerr effects (JASCO, Model K-250). The measurements were performed before and after laser irradiation and subsequent annealing. Figure 5(a) shows the difference spectra for the Faraday rotation angle as a function of wavelength. In the spectrum (a) for a typical condition (annealing at 450 °C for 30 min), a large negative enhancement of the Faraday rotation angle is observed in the blue and ultraviolet regions. One can also find a negative peak at 407 nm in wavelength, which is directly related to the LSPR associated with Al NPs. It should be noted that such negative enhancement due to LSPR is caused by coupling with the ferromagnetic magneto-optical response [2, 7, 8]. Figure 5(b) shows the external magnetic field dependence of Faraday rotation angle at the wavelength of 400 nm at room temperature. The rotation angle subtracted with the diamagnetic contribution of the glass matrix shows the negative rotation which is saturated at fields higher than 10 kOe.

#173803 - $15.00 USD Received 3 Aug 2012; revised 9 Oct 2012; accepted 12 Oct 2012; published 5 Dec 2012

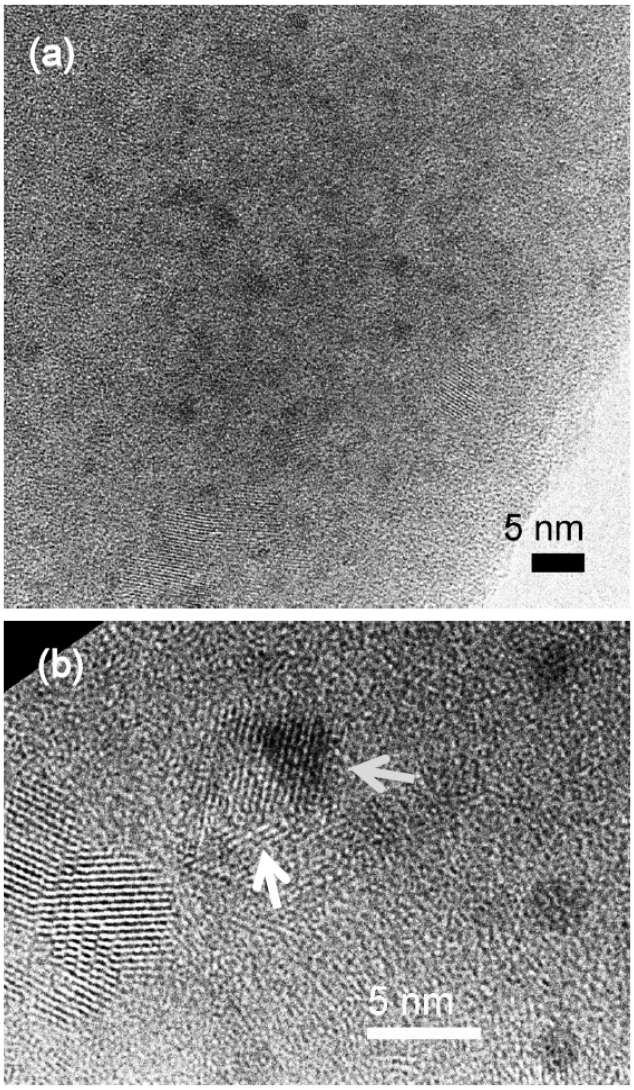

Fig. 4. (a) Bright-field TEM images taken for the glass sample irradiated and annealed at 550 °C for 30 min. (b) Magnified view of nanocomposite structures.

This also suggests that the ferrimagnetic contribution is present due to superparamagnetic NPs, such as magnetite. In contrast, we measured the Faraday effect of the glass doped only with α-Fe_2O_3 that was prepared in our previous paper [21] for comparison. This sample showed a significant enhancement of magnetization at room temperature, although it exhibited no LSPR absorption peak in the optical spectrum. As shown in the spectrum (f), the Faraday effect is not enhanced and shows no negative peak, which indicates that the magneto-optical response due to the ferrimagnetic magnetite NPs was plasmonically enhanced only in the presence of metalic Al NPs. The coupling between the Faraday effect and the plasmon resonance was investigated for different sample conditions. In Fig. 5(a), the difference spectra have been fitted using Gaussian functions. Following background subtraction, the best fits are shown in Fig. 5(c) In the case of (b) the longer annealing time or (c) the higher annealing temperature, it can be seen that the negative peak undergoes a red shift. On the other hand, a blue shift is clearly observed in the case of (d) the lower scanning speed or (e) the higher pulse energy. These results are explainable in terms of a change in the size of plasmonic NPs,

#173803 - $15.00 USD Received 3 Aug 2012; revised 9 Oct 2012; accepted 12 Oct 2012; published 5 Dec 2012

and are consistent with the shift of the LSPR absorption peaks. It can thus be concluded that the enhancement of the Faraday rotation angle is primary due to the LSPR.

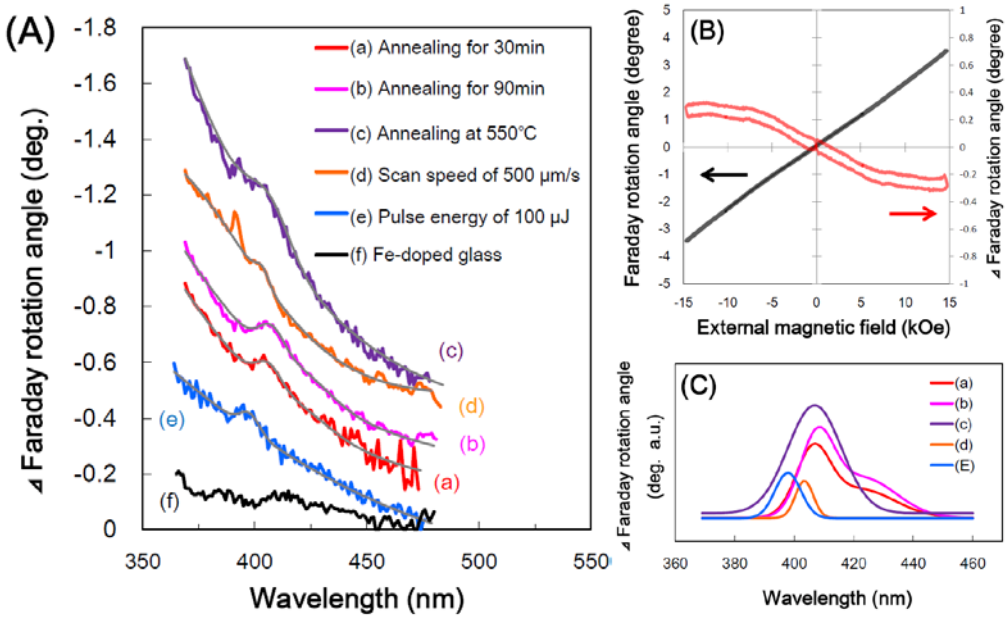

Fig. 5. (A) Difference spectra in Faraday rotation angles for the glass irradiated and annealed (a) at 450 °C for 30 min, (b) at 450 °C for 90 min, (c) at 550 °C for 30 min, (d) at 450 °C for 30 min with a scanning speed of 500 μm/s, and (e) at 450 °C for 30 min with a pulse energy of 100 μJ/pulse. Solid lines show Gaussian fit profiles. (B) Faraday rotation angle and that subtracted with diamagnetic contribution of glass matrix as functions of external magnetic field. (C) The best fits, from which the backgrounds are subtracted, were summarized.

4. Conclusions

A space-selective control of the optical properties, magnetism, and magneto-optical response have been demonstrated using an infrared fs-laser beam focused within transparent glass doped with both α-Fe_2O_3 and Al. The laser irradiation and post-annealing induced the precipitation of Al NPs exhibiting LSPR absorption at around 400 nm, in addition to a ferrimagnetic spinel Fe-oxide nanocrystalline phase. This led to a significant increase in the saturation magnetization at room temperature. In the region surrounding the focal point, atomic diffusion and photoreduction of the dopants occurred, resulting in the formation of plasmonic and ferrimagnetic NPs, respectively. An enhancement of the Faraday effect was also observed together with a negative peak in the magneto-optical spectra at a wavelength corresponding to the LSPR peaks in the optical absorption spectra. The shift of the peak in the Faraday rotation spectra is consistent with that for the LSPR absorption peak, and can be explained in terms of changes in the size of plasmonic NPs. These experimental results indicate a direct coupling between the ferrimagnetic high Faraday rotation and the LSPR, suggesting the space-selective precipitation of nanocomposites consisting of ferrimagnetic magnetite NPs and plasmonic Al NPs. A potential application of this processing method is the structuring of magneto-optical materials for novel magnetic devices such as three-dimensional high-density magnetic recording devices and micro-optical isolators. In addition, since the elements Al and Fe are ubiquitous and inexpensive, this method is an attractive approach for practical plasmonic applications.

#173803 - $15.00 USD Received 3 Aug 2012; revised 9 Oct 2012; accepted 12 Oct 2012; published 5 Dec 2012

Acknowledgment

This work was financially supported by a Grant-in-Aid for Young Scientist (B, No. 20860095) from the Ministry of Education, Culture, Sports, Science, and Technology (MEXT), Japan, and by the Murata Science Foundation, and by the Nippon Sheet Glass Foundation for Materials Science and Engineering.

#173803 - $15.00 USD Received 3 Aug 2012; revised 9 Oct 2012; accepted 12 Oct 2012; published 5 Dec 2012